

PMMA/충격보강제 블렌드의 몰폴로지 및 유변학적 성질에 관한 연구

주용락 · 오주석
한화그룹종합연구소
(1997년 11월 21일)

Morphological and Rheological Studies of PMMA/Impact Modifier Blends

Yong Lak Joo and Joo Seok Oh

Hanwha Group Research and Engineering Center, 6 Shinsung-dong, Yusung-ku, Daejeon 305-345, Korea
(Received November 21, 1997)

요 약

다층 구조를 갖는 고무/아크릴 충격보강제가 poly(methyl methacrylate) (PMMA)/충격보강제 블렌드의 몰폴로지와 유변학적 성질에 미치는 영향을 고찰하였다. TEM으로 측정된 블렌드 내의 충격보강제 몰폴로지는 그 함량에 관계없이 균일한 크기의 구형을 이루는 것으로 나타났으며, 파괴 단면의 SEM 측정으로부터 충격보강제와 매트릭스 수지와의 강한 결합력을 확인할 수 있었다. 블렌드의 유변물성 측정실험에서는 충격보강제 함량이 복합 점도에 크게 영향을 준 반면, capillary rheometer로부터 얻은 정상상태 점도에는 별 영향을 주지않음이 확인되었다. 특히, 동적응력 실험의 고진동 주파수 영역에서는 일정 충격보강제 함량이상 일때 충격보강제 자체의 점도와 근사해졌으며, 이와 같은 현상을 충격보강제의 shell 분자 상호간 또는 매트릭스 분자와의 엉킴에서 비롯되는 물리적인 상호 작용 측면에서 설명해보았다. 또한, 실험 결과를 Palierne[16]의 비상용성블렌드계의 이멀전 모델과 비교한 결과, 상당한 차이를 확인할 수 있었으며, 이러한 차이는 위에서 언급한 shell 분자 상호간 또는 매트릭스 분자와의 엉킴에 기인한다고 추정된다.

Abstract—The effects of a multi-layered rubber-acrylic impact modifier on the morphology and rheology of poly(methyl methacrylate) (PMMA)/impact modifier (IM) blends are investigated. Morphologies of the blends obtained by TEM show that the size of the impact modifier domains is uniform and unchanged, and the shape remains spherical, although the IM concentration is increased. It is also shown that the fracture surfaces of the blends directly examined by SEM have indication of strong adhesion between the IM particles and the PMMA matrix. Our results of the rheological study reveal that the complex viscosity of the blends is strongly influenced by the content of the modifier, while the addition of the impact modifier hardly changes the apparent viscosity measured in the capillary experiments. We note that when high frequency is applied in the oscillatory shearing experiments, the complex viscosity of the blend abruptly increases and approaches that of impact modifier, as the IM concentration reaches a certain critical value. The experimentally observed effects of impact modifier on the rheology of the PMMA/IM blends are interpreted considering possible physical interactions via entanglements of the acrylic shell molecules with the PMMA matrix molecules or other shell molecules. In addition, the dynamic shear measurements are compared with an emulsion model for immiscible blends by Palierne [12]. Significant deviations between the results from the dynamic shear experiments and the emulsion model applied are observed, and this may be due to the strong entanglements of the acrylic shell of the impact modifier particles with the PMMA matrix molecules or other shell molecules.

Keywords: Impact modifier, PMMA blend, Oscillatory shearing, Emulsion model, Entanglements

1. Introduction

It has long been known that amorphous polymers can exhibit two different material characteristics. Some, like poly(methyl methacrylate) (PMMA) and polystyrene (PS) are hard, rigid, but brittle at room temperature, while others, for example polybutadiene, polyethyl acrylate and polyisoprene, are soft, flexible, and rubbery materials. Impact modifiers are in general rubbery materials that impart such toughness when blended with brittle plastics[1,2].

Numerous plastic/impact modifier systems have been

studied and it has been reported that the degree of impact strength is influenced by a variety of factors including the content, the type, and the particle size of impact modifier [3-7]. The addition of large quantities of core-shell structured impact modifier has been found useful in brittle polymers.

In a glassy, initially transparent plastic the presence of the microscopic rubber particles results in a loss of transparency. This is due to light scattering by the rubber particles which are typically within the size range of 0.5~20 μm [8]. Therefore, it is of great concern to sustain optical

properties of toughened polymers in applications requiring transparency. The effect can be minimized and surface gloss maintained by making the particle size small ($<0.2 \mu\text{m}$) and by keeping the particles well dispersed[9]. For PMMA, which has excellent transparency as one of its main attributes, special rubbery particles have been developed so that toughening can be achieved without a significant decrease in its transparency[10,11]. We also developed a three-layered impact modifier system, which is composed of seed, core, and shell, to enhance impact strength without degrading optical properties. In the modified toughening particles we employed, the acrylic seed is embedded inside the rubbery core such that both the deformation of impact modifier particles in shearing flows and the change in optical properties of the blend can be greatly reduced. Meanwhile, the acrylic molecules which have the identical chemical structure as the matrix molecules are grafted on to the rubbery core in the impact modifier so that the impact modifier and the acrylic matrix can be physically interacted.

Macroscopically, our PMMA/IM blends are immiscible because the rubbery core of the impact modifier and the matrix have dissimilar chemical structures, while the acrylic shell, which is grafted on to the core, and the matrix have identical chemical structure and they can entangle each other. Therefore, one can easily surmise that the addition of the impact modifier with such a structure results in a formation of a microscopically complex morphology and as a consequence the blend may also exhibit complex rheological behaviors. Later we will demonstrate that our PMMA/impact modifier system generates spherical, mono-dispersed impact modifier domains regardless of the content of the modifier, while the resulting rheologies of the blends are strongly influenced by the type of flows applied and the content of the modifier. This macroscopically simple blend system leads to easier investigation of the isolated effect of the impact modifier on the rheology of the blend, which may arise from the dynamics of molecules at the interfacial regions, and the discrete effect of such physical interactions including possible entanglements between the shell molecules grafted on to the rubbery core in the impact modifier and the matrix molecules on the rheology can be manifested.

The purpose of the present communication is twofold. First, we examine the effects of the impact modifier content on the morphology of the PMMA/IM blends. TEM (transmission electron microscopy) and SEM (scanning electron microscopy) are employed to probe the microstruc-

ture of the blends with various impact modifier compositions. Micrographs that can elucidate the size, shape and distribution of the impact modifier particles in the blends at various blend compositions and some evidences for strong adhesion between the impact modifier domain and the matrix are presented.

After examining the effects of the impact modifier on the morphology, we turn to the second purpose of this communication in which the effects of the impact modifier content on the rheology of PMMA/IM blends are presented. It should be noted that the impact modifier exhibits the viscoelastic behavior of a rubbery material, while PMMA matrix shows that of a typical polymer melt. Therefore, we can easily picture that the addition of impact modifier would significantly alter the rheological properties of the PMMA/IM blend. The experimentally observed effects of impact modifier on the rheology of the blends are then interpreted considering the physical interactions via entanglements of the acrylic shell molecules with the PMMA matrix molecules. Furthermore, the dynamic shear measurements are compared with an emulsion model for immiscible blends by Palierne[12].

2. Experimental

2.1. Materials

PMMA "HY020" produced by Hanwha Chemical Corp. was used as the polymer matrix. It is characterized as melt flow rate (MFR)=1.8 g/10 min (ASTM D 1238 under 3.8 Kg load at 230°C), density=1,190 Kg/M³ (ASTM D 792), $M_w=121,985$, and $M_n=58,939$.

Sequential emulsion polymerization was used to prepare three-layer toughening particles. First, a copolymer of methyl methacrylate-methyl acrylate (MMA-MA) which acts as a rigid seed was polymerized and partially cross-linked. A copolymer of butyl acrylate-styrene (BA-S) was then employed as a rubbery core. This rubbery core was also partially cross-linked for ease of handling and thermal stability during the melt blending. We can anticipate that the presence of a rigid, acrylic seed in the core will 1) reduce the deformation of the impact modifier domains in shearing flows, 2) provide an uniform size distribution of the modifier particles, and 3) help with retaining the optical properties of the blend. Finally, copolymers of methyl methacrylate-methyl acrylate (MMA-MA) which form the outer shell to interact with the PMMA matrix were grafted on to the core. The average grafting efficiency determined by thin layer chromatography and flame ionization de-

Table 1. Properties of PMMA/IM blends

Impact Modifier Concentration (wt%)		0	10	20	30	40	100
Impact Modifier Concentration (vol%)		0	11	21.76	32.28	42.58	100
Melt Density(kg/m ³)		1,070	1,066	1,040	1,040	1,040	1,040
Melt Flow Rate (g/10 min)		1.78	1.46	1.02	0.66	-	-
Compressed Sheet (3 mm thick)	Light Transmission	90.0	86.3	86.3	86.6	87.1	89.9
	Haze	5.11	5.78	5.07	5.03	6.00	10.27
Extruded Film (100 μm thick)	Light Transmission	92.7	92.6	92.6	92.6	-	-
	Haze	0.1	3.6	3.2	3.7	-	-

pector was found to be about 30% [13] and the molecular weight of ungrafted shell molecules ranged from 60,000 to 100,000. The average size of the impact modifier determined by the dynamic light scattering experiment was about 0.18 μm.

2.2. Preparation of Poly(methyl methacrylate)/Impact Modifier Blends

HY020 and the core-shell structured rubber-acrylic impact modifier were introduced in the intermeshing corotating twin screw extruder (Leistritz, barrel diameter=27 mm, L/D=38). The screw rpm was 250 and the barrel temperatures ranged from 200 -240°C. Six blends were prepared with varying impact modifier concentration from 5 to 40 wt%.

2.3. Methods

Morphology versus the composition of the PMMA/IM blends was assessed on compressed sheets using TEM and SEM. TEM was employed to probe the microstructure of the impact modifier phase in the PMMA/IM blends. In TEM study, the sections were adequately stained with osmium tetroxide (OsO₄) after being cut perpendicularly to the plain of the compression. Meanwhile, the fractured surfaces of the PMMA/IM blends were directly examined by SEM to assess adhesion between the impact modifier domains and the PMMA matrix.

For the rheological study of the blends, both steady and oscillatory shearing properties of the PMMA/IM blends are measured at various temperatures, namely at 200°C, 220°C, and 240°C using a twin-bore capillary rheometer (Rosand RH7-8/2, D=1.0 mm, L=25 mm, and l=2.5 mm, entrance angle=90°) and a parallel-plate rheometer (Rheometrics Dynamic Spectrometer, 25 mm diameter plates with

a 2.0 mm gap between the plates), respectively. In the steady shear viscosity measurements, the results were both Bagley and Rabinowitsch corrected. In the oscillatory measurements, different oscillatory strains range from 2.5% to 15% were applied. In all cases, it was verified that the viscoelastic response was in the linear regime.

Optical properties including light transmission and haze were measured before and after extruding the blends into thin films. Some properties of the PMMA/IM blends are listed in Table 1 [14].

3. Theoretical background

3.1. Emulsion Models for Immiscible Blends

It has long been seeking to getting model predictions for the rheological behavior of an immiscible blend in which the minor phase is usually dispersed in the form of spherical inclusions in the major phase. The starting point for models describing the rheology of such polymer blends are emulsion models as presented, for example, by Oldroyd[15] and Choi and Schowalter[16]. These models deal with emulsions and suspensions of two Newtonian fluids and predict an elastic contribution in the rheological response which can be attributed to the form relaxation of the inclusions[17]. The characteristic time of this process depends on the radii of the inclusions and on the interfacial properties between the blends' components.

The influence of the form relaxation can also be observed in polymer blends. In 1990, Palierne published a model which leads to the following equation relating the linear viscoelastic material functions of the blend and its components to the interfacial properties and the sphere-size distribution of the inclusions[12,18-20].

$$G_b^*(\omega) = G_m^*(\omega) \frac{1 + 3 \sum_i \phi_i H_i(\omega)}{1 - 2 \sum_i \phi_i H_i(\omega)} \quad (1)$$

with

$$H_i \left(\omega, \frac{R_i}{\alpha} \right) = \frac{4 \frac{\alpha}{R_i} [2G_m^*(\omega) + 5G_d^*(\omega)] + [G_d^*(\omega) - G_m^*(\omega)] [16G_m^*(\omega) + 19G_d^*(\omega)]}{40 \frac{\alpha}{R_i} [G_m^*(\omega) + G_d^*(\omega)] + [2G_d^*(\omega) + 3G_m^*(\omega)] [16G_m^*(\omega) + 19G_d^*(\omega)]} \quad (2)$$

where $G_m^*(\omega)$, $G_d^*(\omega)$, and $G_b^*(\omega)$ are the complex shear moduli of the matrix, the dispersed phase, and the blend, respectively. α is the interfacial tension which is the sole

parameter describing the interfacial properties between the components, and denotes the volume fraction of the inclusions with radius R_i . The entire volume fraction of the dispersed phase is $\phi = \sum \phi_i$.

Meanwhile, Gramspacher and Meissner used an extension of the model of Choi and Schowalter in which the contribution caused by the viscoelastic properties of the components and the interfacial tension are separately considered[21]. Doi and Ohta suggested an interesting model describing the time evolution of interfacial area and its anisotropy in a given flow field in which the constituents consist of Newtonian fluids and have equal viscosities[22,23]. The stresses arising as a consequence of interfacial tension were assumed in their theory to change with the deformation and relaxation of the interface during the flow (drop deformation, coalescence, and breakup). The theory of Doi and Ohta was modified by Lee and Park to account for a mismatch in the viscosities of the polymers and an additional kinetic equation associated with the relaxation of the interface due to droplet breakup[24].

Later, we will demonstrate that our PMMA/impact modifier system generates spherical, mono-dispersed impact modifier domains regardless of the content of the modifier. As a result, the effects of break-up, coalescence, and size distribution of the dispersed phase on the rheology of the blend can be greatly reduced. This simple blend system leads to easier investigation of the effect of impact modifier on the rheology of the blend, and the complex effects of droplet breakup and coalescence on the rheology of the blends can be disregarded. Therefore, the simple emulsion model for immiscible blends by Palierne [Eq. (1)] will be applied to predict the dynamic shear properties of the PMMA/IM blends.

4. Results and Discussion

4.1. Morphology of PMMA/IM blends

4.1.1. TEM (Transmission Electron Microscopy)

Transmission electron microscopy techniques offer the best image resolution of all of the microscopy techniques and structural information relating the size and shape of the dispersed phase is available. Dispersed phase structures can often be imaged and domains observed and quantified over a size range from less than 10 nm up to 1 μm [25]. Fig. 1 shows the resulting morphologies of the PMMA/IM blends at various blend compositions obtained by TEM imaging to show the seed-core-shell microstructure. The dark areas represent the core parts of the core-

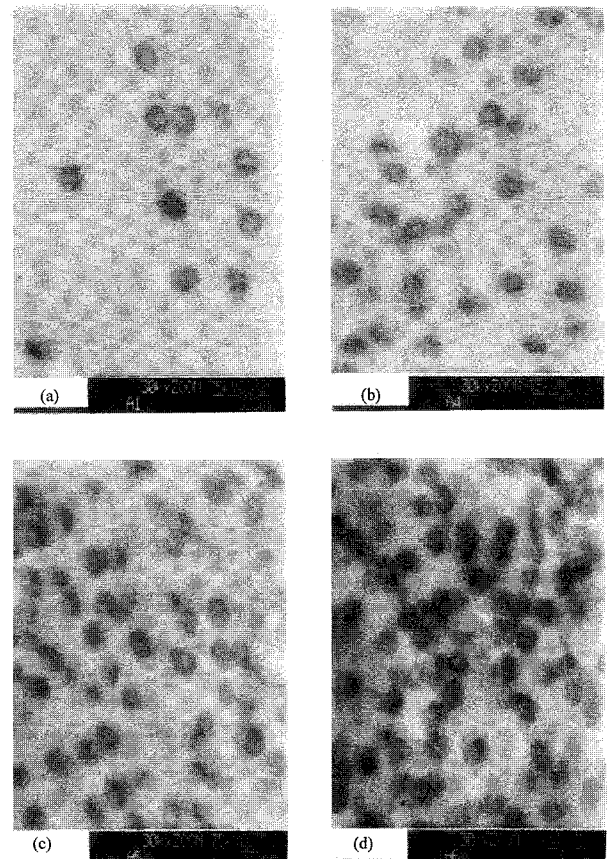


Fig. 1. Transmission electron micrographs of PMMA/impact modifier blends with various impact modifier concentrations ($\times 30,000$). (a) 5 wt%, (b) 20 wt%, (c) 30 wt %, and (d) 40 wt%. The dark areas represent the core parts of the core-shell impact modifier, while the background is the PMMA matrix. The bright areas inside the dark rubbery cores represent the acrylic seeds embedded to reduce its deformation in shearing flows.

shell impact modifier, while the background is the PMMA matrix. We note that the bright areas inside the dark rubbery cores represent the acrylic seeds embedded to reduce its deformation in shearing flows. It is observed that at low content of IM, the IM domains are disconnected and well separated from one another (see Fig. 1a). As the IM concentration increases, the IM domains start to interconnect with one another [Fig. 1b and c], and eventually form a network that pervades the entire matrix as shown in Fig. 1d. It should be noted that the size of the impact modifier particles is uniform and unchanged, and the shape remains roughly spherical, although the IM concentration is increased. It is also found that the average size of IM particles are about 0.2 μm , which is in good agreement with the value obtained by the dynamic light scattering experiment.

4.1.2. SEM (Scanning Electron Microscopy)

Scanning electron microscopy is a very popular tech-

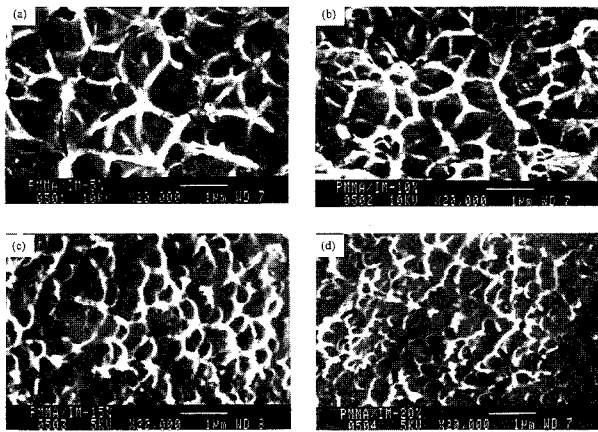


Fig. 2. Scanning electron micrographs of fractured surfaces of PMMA/impact modifier blends with various impact modifier concentrations ($\times 20,000$). (a) 5 wt%, (b) 10 wt%, (c) 15 wt%, and (d) 20 wt%. The dark areas in each micrograph represent ruptured parts of IM and PMMA, while the bright areas represent the remaining PMMA matrix.

nique, which can provide $100\times$ better resolution than optical microscopy and surfaces are easy to prepare. The large depth of the field is the major advantage as uneven surfaces with vertical differences $100\times$ the resolution still produce focused images[26]. The impact modifier phase in the PMMA/IM blends with various impact modifier concentration which is directly examined by SEM study of fractured surfaces is shown in Fig. 2. The dark areas in each micrograph represent ruptured parts of IM and PMMA, while the bright areas represent the remaining PMMA matrix. It is seen that the fracture surfaces of each blend has indication of strong adhesion between the IM particles and the PMMA matrix: The impact modifier particles in each micrograph do not appear to be dislodged from the PMMA matrix. This implies that the acrylic shell of the IM particles adheres to the PMMA matrix, reinforcing the interface. It should also be noted that the size of the ruptured parts becomes smaller and eventually reaches that of the impact modifier particles as the IM content is increased. This may indicate that the impact strength of the blend ceases to increase if the IM content reaches a certain critical value[27].

From the morphological study of the PMMA/impact modifier blends with various blend compositions, it is observed that the size of the impact modifier particles is uniform and unchanged, and the shape remains spherical, although the blend composition is changed. It is also shown that the fracture surfaces of the blends directly examined by SEM study have indication of adhesion between the IM particles and the PMMA matrix.

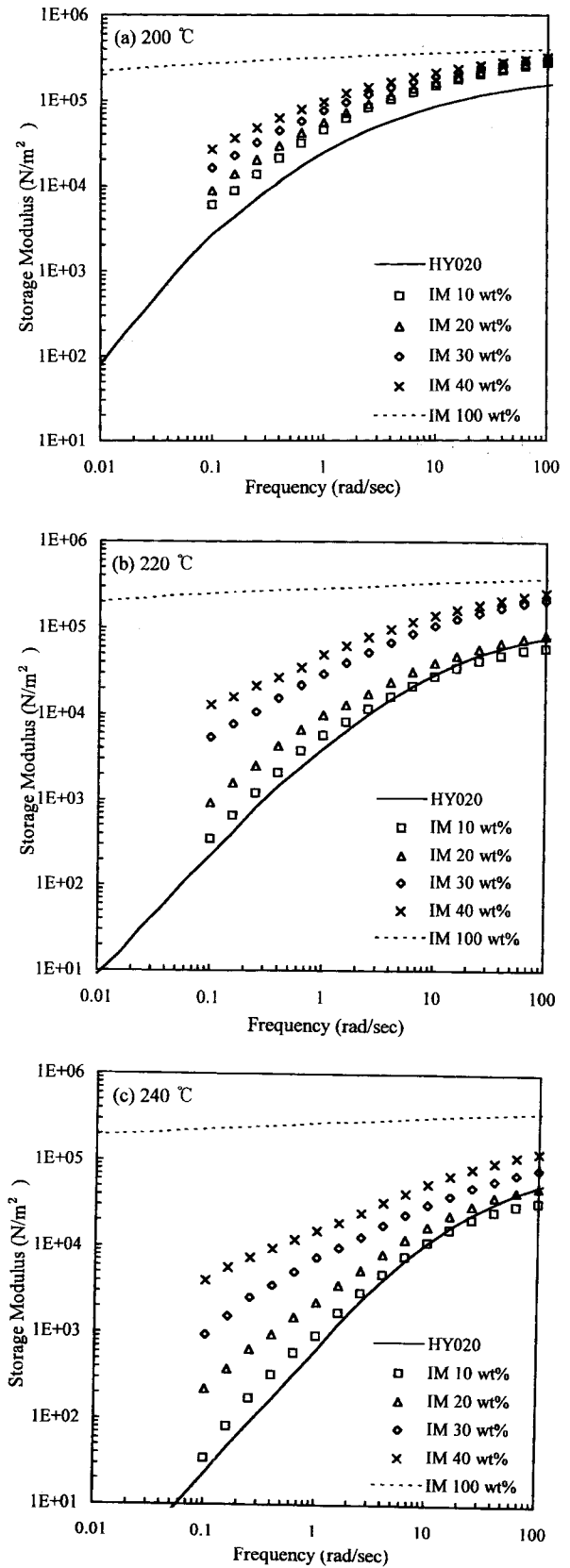


Fig. 3. Plots of $\log G'$ vs. ω for PMMA/IM blends at various temperatures. (a) at 200°C , (b) at 220°C , and (c) at 240°C .

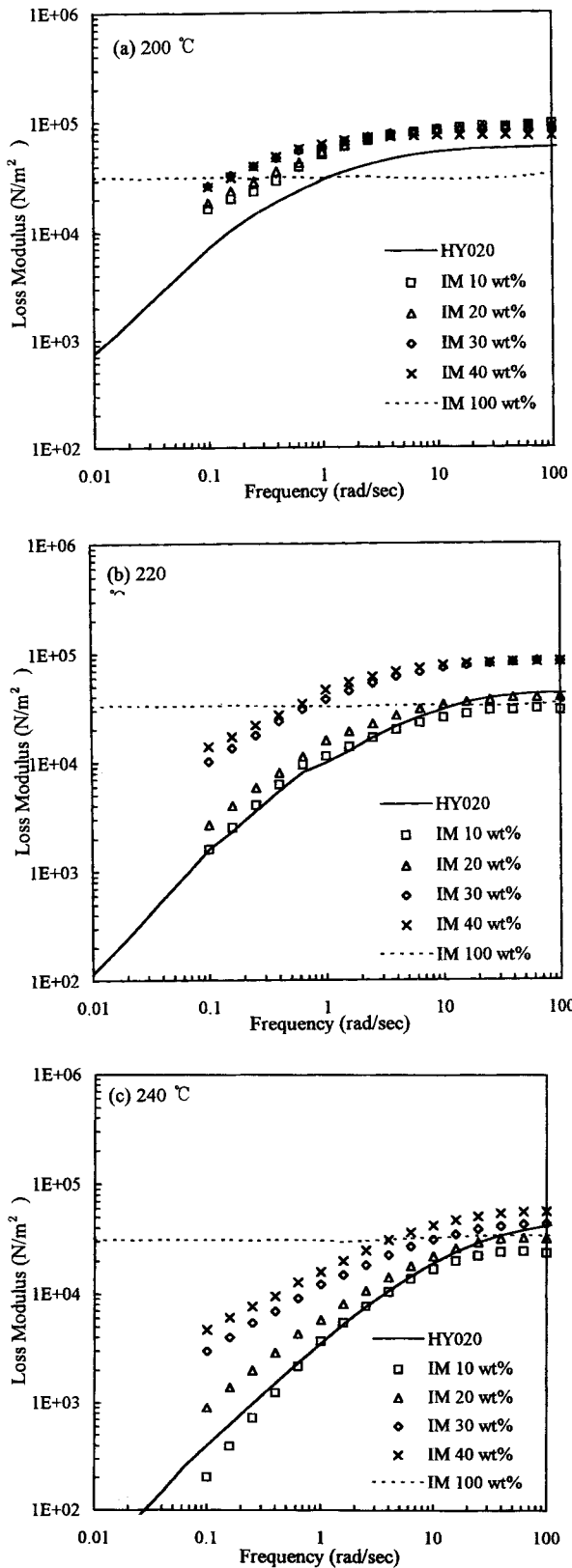


Fig. 4. Plots of log G'' vs. ω for various PMMA/IM blends at three different temperatures. (a) at 200°C, (b) at 220°C, and (c) at 240°C.

4.2. Rheology of PMMA/IM blends

4.2.1. Oscillatory Shearing Flow

In oscillatory shear flow the dynamic storage modulus G' can be considered as the amount of energy stored and the loss modulus G'' as the amount of energy dissipated in a viscoelastic fluid[28].

Figs. 3 and 4 illustrate the dependence of the storage and loss moduli on blend composition at three different temperatures. It is observed that the impact modifier exhibits the viscoelastic behavior of a rubbery material (i.e. constant G' and G''), while PMMA matrix shows that of a typical polymer melt ($G' \sim \omega^2$, $G'' \sim \omega^1$) in the low frequency regime. It is observed that there is a noticeable increase in both loss and storage moduli when the impact modifier content exceeds a certain critical value. We note that in the high frequency regime the loss modulus of the blend becomes even higher than those of the two constituent components as the impact modifier concentration exceeds a certain critical value, while the storage modulus of all the blends lie between those of the constituent components. This complex behavior of storage and loss moduli on blend composition may be primarily due to the possible physical interactions between the impact modifier and the PMMA matrix via entanglements of acrylic shell molecules with the acrylic matrix molecules or other shell molecules: Based on the values of the entanglement molecular weight for PMMA in their binary blends by Onogi *et al.* ($M_e=6,700-13,100$)[29], the molecular weights of the matrix and the shell molecules are several times greater than the value of M_e and therefore the matrix and the shell molecules can easily be entangled. As the impact modifier concentration is increased, the acrylic shell of the impact modifier starts to interact and entangled with more PMMA matrix molecules and other shell molecules, and thus the whole PMMA/IM blend may eventually begin to behave like impact modifier as the impact modifier content exceeds a certain critical value. In addition, the dependence of both storage and loss moduli on the frequency decreases as the impact modifier content is increased.

Fig. 5 gives plots of the complex viscosity of PMMA/IM blends, $|\eta^*|$, versus frequency ω at three different temperatures. It is shown that the complex viscosity increases as the content of impact modifier is increased.

It is worth noting that the complex viscosity of the blend at high frequency abruptly increases and approaches that of impact modifier, as the impact modifier concentration reaches a certain critical value. We suspect that this prominent increase in the complex viscosity may primarily

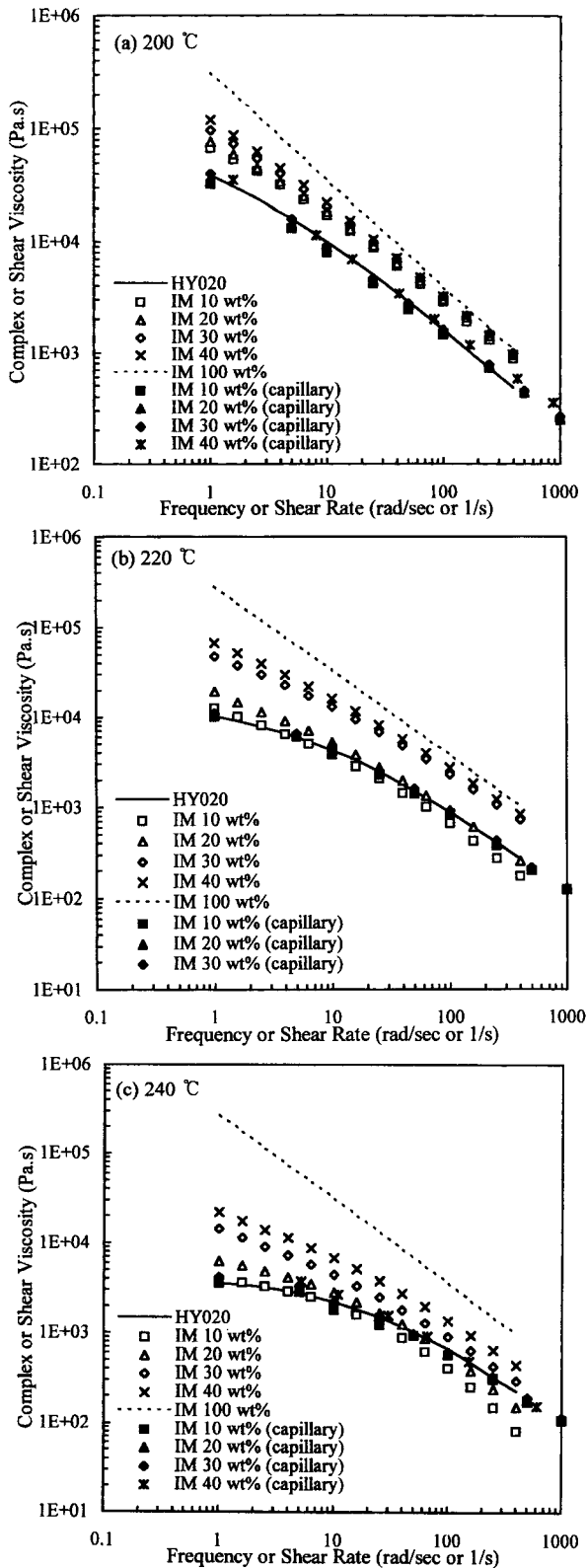


Fig. 5. Comparison of the complex viscosity from the plate-and-plate rheometer with apparent shear viscosity obtained from the capillary rheometer. (a) at 200°C, (b) at 220°C, and (c) at 240°C. Complex viscosity and apparent shear viscosity of various blend compositions are shown at each temperature.

be owing to the strong interactions between the impact modifier particles and the PMMA matrix. In particular, high values of complex viscosity in the high frequency regime may be associated with the recent observations of extreme shear-induced brush thickening of solvent-filled polymer brushes under oscillatory shear by Klein *et al.*[30-32]. If we view the acrylic shell molecules as polymer brushes tethered on the rigid surface (the core), the shell molecules can greatly be extended due to the shear-induced diffusion as suggested by Doyle *et al.* using Brownian dynamics simulation[33], and this thickening of the shell molecules may lead to a higher degree of entanglements with the matrix molecules or other shell molecules.

This critical concentration of impact modifier above

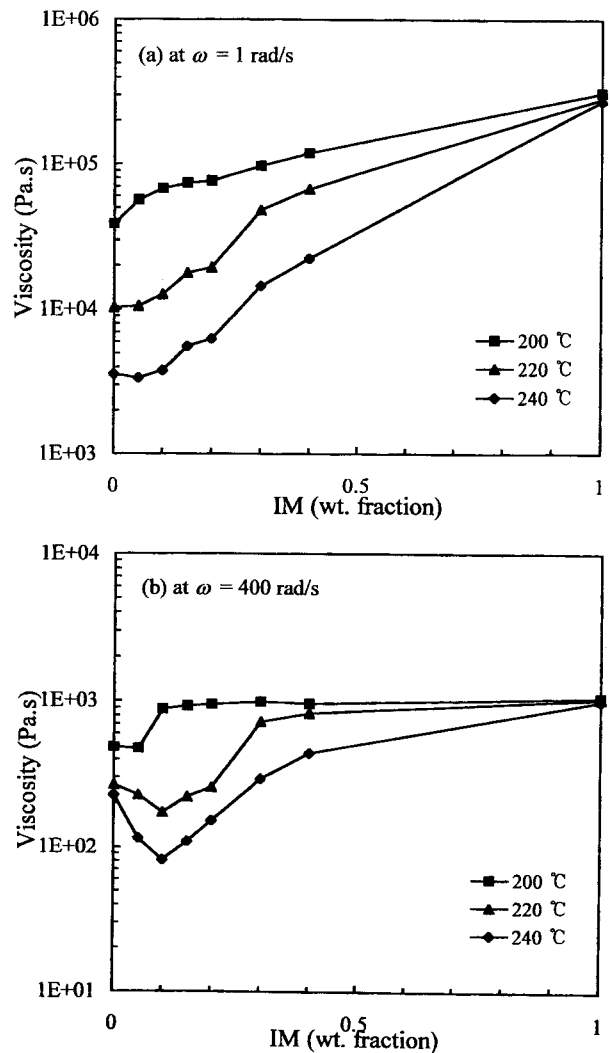


Fig. 6. Complex viscosity vs. blend composition curves at two different frequencies, (a) $\omega=1$ rad/sec and (b) $\omega=400$ rad/sec. Viscosity of various blend composition is shown at three different temperatures.

which shear viscosity of the blends in the high frequency regime approaches that of impact modifier is found to increase with increasing temperature as shown in Fig. 5: The critical concentrations of impact modifier at 200°C, 220°C, and 240°C are 10 wt %, 30 wt %, and above 40 wt %, respectively. The increase in the critical concentration of impact modifier with increasing temperature may be due to weak entanglements between the impact modifier and the PMMA matrix at elevated temperatures. One would expect that the weaker the extent of interactions (i.e. less entanglements) between the impact modifier domains and the PMMA matrix at elevated temperatures, the higher IM content is required to make the whole PMMA/IM blend behave like impact modifier.

The effect of impact modifier on the complex viscosity at given frequencies ($\omega=1$ rad/sec, $\omega=400$ rad/sec) can be seen in the complex viscosity-blend composition curves (see Fig. 6). It is also seen that the shear viscosity of the blend at high frequencies ($\omega=400$ rad/sec) abruptly increases and approaches that of impact modifier, as the IM concentration reaches a certain critical value. It is also worth noting that when high frequency ($\omega=400$ rad/sec) is applied at elevated temperatures (220 °C and 240°C), the viscosity-blend composition curve goes through a minimum, while the viscosity increases monotonically with blend composition at low frequency ($\omega=1$ rad/sec) as indicated in these graphs. This may indicate that at low frequency impact modifier particles which are well separated one another have relatively little interaction and the impact modifier particles is not extensively deformed. As a result, the viscosity increases monotonically with blend composition at low shear. TEM micrographs in Figure 1 showed that the size of the impact modifier particles is uniform, and the shape remains almost spherical, and we can assume that the morphology of the blend at low frequency would resemble that of the compressed sheet. Meanwhile, in the high frequency regime the impact modifier domains may get easily deformed and aligned in the flow direction as temperature increases. If the impact modifier domains were anchored loosely onto the continuous PMMA matrix because of weak interaction between the shell molecules of the impact modifier and the matrix at higher temperatures, one would expect that the deformation of such domains would require much less forces than those are strongly anchored. Therefore, we suspect that the observed minimum in the shear viscosity in the blends at high temperatures may be attributable to the deformation of the impact modifier domains, when subjected to high-

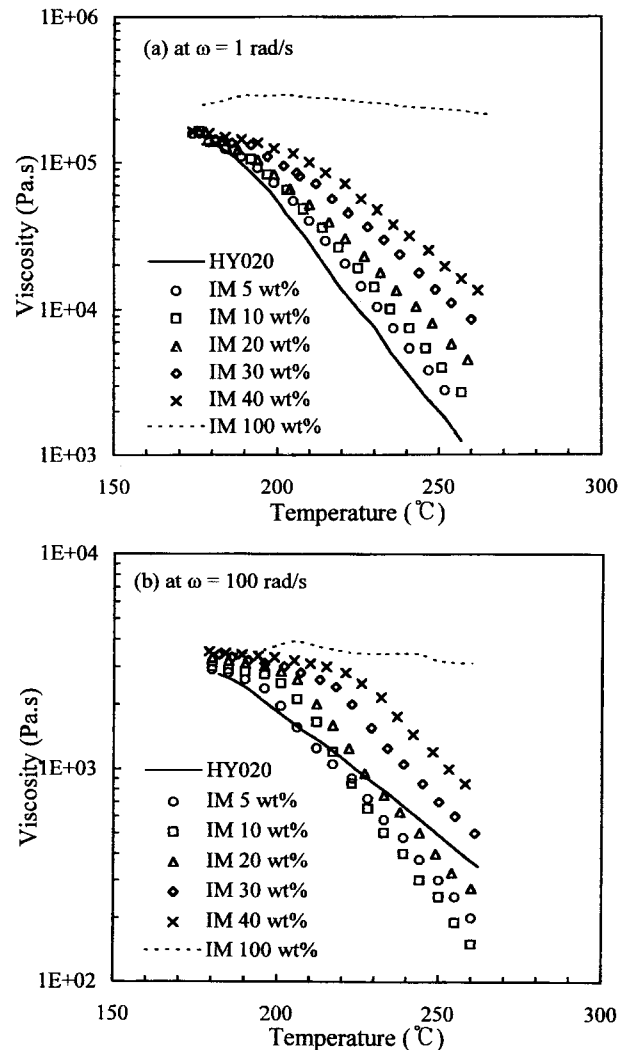


Fig. 7. Complex viscosity vs. temperature curves at two different frequencies, (a) $\omega=1$ rad/sec and (b) $\omega=100$ rad/sec.. The dependence of the viscosity of various blend composition on temperature is shown.

frequency deformation. Further experimental studies aimed at identifying the key factors of the changes in the rheological behavior by modulating the molecular entanglements between IM and the PMMA matrix by changing molecular weights of both the grafted shell and the matrix molecules are underway.

Fig. 7 shows the temperature dependence of the complex viscosity of the blends at two different frequencies ($\omega=1$ rad/sec, $\omega=100$ rad/sec). It is observed that at both frequencies, the complex viscosity of the impact modifier shows little temperature dependence, while that of the PMMA matrix exhibits significant temperature dependence. As a result, the temperature dependence of the complex viscosity steadily decreases as the content of impact modifier is increased. It should be noted that when high frequency is applied ($\omega=$

100 rad/sec), the viscosity of the blends with various blend composition shows little temperature dependence at low temperatures, while it exhibits significant temperature dependence at elevated temperatures. This implies that the physical interaction between the impact modifier particles and the PMMA matrix such as entanglements, and possibly the extent of deformation of the impact modifier domains may strongly depend on both temperature and oscillation frequency.

4.2.2. Steady Shearing Flow

The viscosity of PMMA/IM blends versus shear rate at two different temperatures measured in a capillary rheometer was plotted and compared with the complex viscosity obtained from plate-and-plate rheometer in Fig. 5. It is shown that the shear viscosity hardly changes as the content of impact modifier is increased up to 40 wt%. This is substantially different from the results of oscillatory shearing experiments in which the complex viscosity of the blend exhibits strong dependence on the composition. We attribute these different rheological behaviors in two different shearing flows to different dynamics of entanglements of the acrylic shell molecules with the matrix molecules. In a steady shear flow, the acrylic shell molecules may not be able to extend freely, and thus the slippage between the acrylic shell molecules with the matrix molecules which may lead to a significant reduction in the degree of entanglements can take place. Note that no brush thickening was ever witnessed in steady flow of solvent-filled polymer brushes[34-36].

Further experimental studies aimed at identifying the key factors of the changes in the rheological behavior by modulating the molecular entanglements between IM and the PMMA matrix by changing molecular weights of both the grafted shell and the matrix molecules are underway.

From the rheological study of the PMMA/impact modifier blends with various blend composition, it is inferred that the physical interactions between the impact modifier and the PMMA matrix via entanglements of acrylic shell molecules with the acrylic matrix molecules or other shell molecules are strongly influenced by the changes in blend composition, temperature, and type of shearing flow applied. As a result, both the viscosity and viscoelastic properties of the blends vary to a great extent in a very complex manner with varying blend composition, temperature, and the type of shearing flow applied.

4.3. Comparison of the Dynamic Shear Experiments with the Emulsion Models

The dynamic shear measurements of PMMA/IM blends with different compositions at different temperatures are compared with the emulsion model for immiscible blends by Palierne. The emulsion model by Palierne [Eq. (1)] for the spherical, mono-dispersed impact modifier/PMMA system can be simplified as

$$G_b^*(\omega) = G_m^*(\omega) \frac{1 + 3\phi H(\omega)}{1 - 2\phi H(\omega)} \quad (3)$$

with

$$H_1\left(\omega, \frac{R}{\alpha}\right) = \frac{4\frac{\alpha}{R}[2G_m^*(\omega) + 5G_d^*(\omega)] + [G_d^*(\omega) - G_m^*(\omega)][16G_m^*(\omega) + 19G_d^*(\omega)]}{40\frac{\alpha}{R}[G_m^*(\omega) + G_d^*(\omega)] + [2G_d^*(\omega) + 3G_m^*(\omega)][16G_m^*(\omega) + 19G_d^*(\omega)]} \quad (4)$$

where ϕ denotes the total volume fraction of the inclusions with radius R . It is interesting to note that when the shear is small ($\omega < 1$ rad/sec), the ratio of the modulus of the impact modifier to that of the PMMA matrix is substantially large ($G_d^*(\omega)/G_m^*(\omega) \gg 1$, see Figs. 3 and 4) and Eq. (4) becomes $H(\omega) = \frac{1}{2}$. Therefore, Eq. (3) can be reduced to the following simple equation for the PMMA/IM blends at low shear

$$G_b^*(\omega) = G_m^*(\omega) \left(\frac{1 + \frac{3}{2}\phi}{1 - \phi} \right) \quad (5)$$

Eq. (5) implies that a dispersion of rubbery materials with large values of complex modulus in a viscoelastic matrix can be considered as a system of rigid spheres dispersed in a viscoelastic matrix, and that the interfacial properties play an insignificant role in the viscoelastic behavior of the blend.

Figs. 8 and 9 show the comparison between the dynamic shear measurements of two blends with different compositions at three different temperatures, namely, 200°C, 220°C, and 240°C, and the emulsion model by Palierne [Eq. (3)] and its limiting case for emulsion of hard spheres [Eq. (5)].

It is observed that Palierne model and the hard sphere model are indistinguishable in the low frequency regime ($\omega < 1$ rad/sec), and deviations between two models increase when oscillation frequency or the content of impact modifier is increased, or temperature is decreased. This may be due to the fact that the main assumption leading to Palierne model is that the droplet deformation remains small. It is observed that the agreement with the experimental data is quite poor

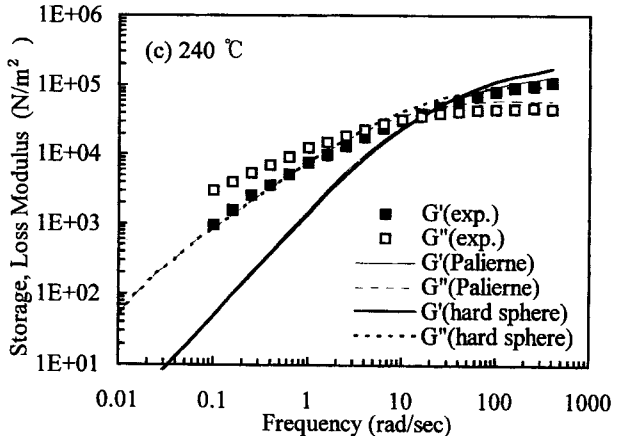
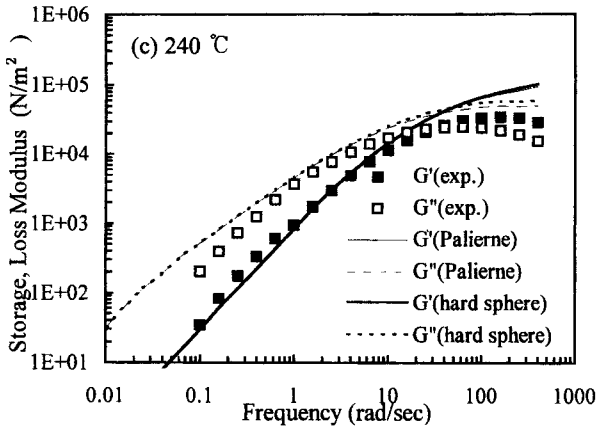
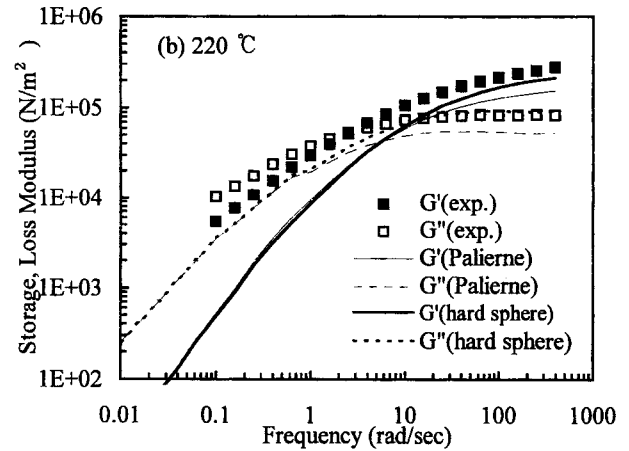
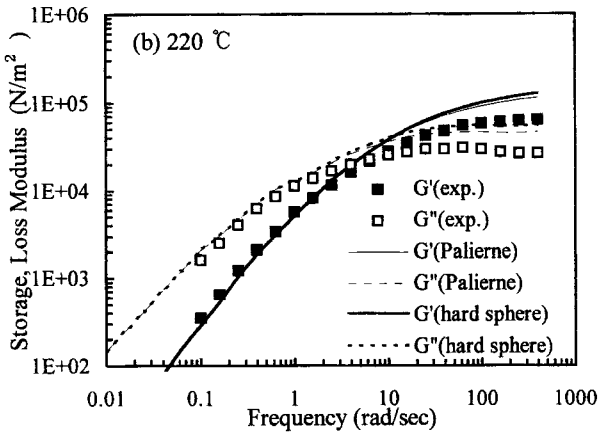
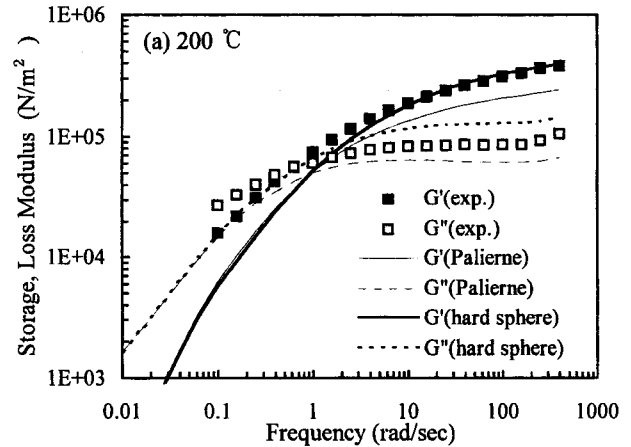
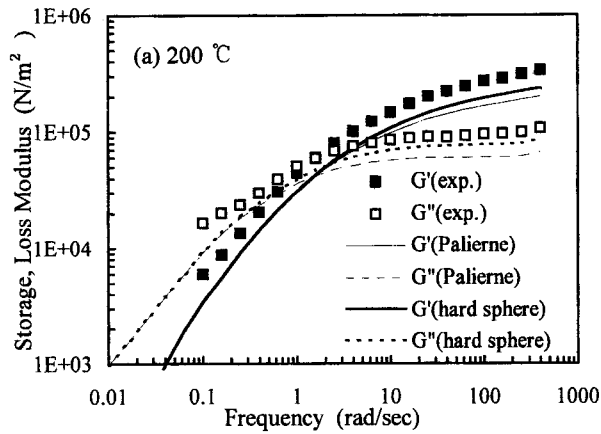


Fig. 8. Comparison of the predictions of the emulsion models with the experimental results for the blend with 10 wt% of impact modifier at three different temperatures: (a) 200°C, (b) 220°C, and (c) 230°C.

for any value of $\frac{\alpha}{R}$, although the coefficient $\frac{\alpha}{R}$ was used as an adjustable parameter in Eq. (3) to attain the best fit with our experimental data in the high frequency regime. We note that when temperature is low and thus the interactions between the impact modifier and the matrix are strong, the model predictions are significantly lower than the results from the dynamic shear experiments in the en-

Fig. 9. Comparison of the predictions of the emulsion models with the experimental results for the blend with 30 wt% of impact modifier at three different temperatures: (a) 200°C, (b) 220°C, and (c) 230°C.

tire frequency regime. We attribute this difference to the physical interactions via entanglements of the acrylic shell molecules with the PMMA matrix molecules which are not taken into account in the emulsion models applied. It is observed that these deviations decrease with increasing temperature possibly due to decrease in the physical interactions between the impact modifier and the matrix. It

should also be noted that the models underpredict the high frequency behavior of the blend at low temperature, while they overpredict the high frequency behavior of the blend at higher temperatures.

Meanwhile, at the high volume fraction of impact modifier, deviations between the results from the dynamic shear experiments and the model prediction are further increased in the low frequency regime. Besides the fact that the physical interactions between the impact modifier and the matrix increase with increasing the impact modifier content, other types of interactions can take place at high volume fractions because the acrylic shell molecules of impact modifier can contact with each other.

It should be noted that significant deviations between the results from the dynamic shear experiments and the emulsion model in which only hydrodynamic interactions are included are observed, and this may be due to the strong interactions between the acrylic shell of the impact modifier particles and the matrix which are not taken into account in the emulsion models applied.

5. Conclusions

We have presented the effects of a seed-core-shell structured rubber-acrylic impact modifier on the morphology and rheology of PMMA/impact modifier (IM) blends. First, morphology versus the composition of the blends was assessed using TEM (transmission electron microscopy) and SEM (scanning electron microscopy). It is observed that the size of the impact modifier particles was uniform and unchanged, and the shape remained spherical, although the IM concentration was increased. It was also shown that the fracture surfaces of the blends directly examined by SEM study had indication of adhesion between the IM particles and the PMMA matrix.

For the rheological study, both steady and oscillatory shearing properties of the eight PMMA/IM blends were determined. Our results revealed that the complex viscosity of the blends from the oscillatory shearing experiments was strongly influenced by the content of the modifier, while the addition of the impact modifier hardly changed the apparent viscosity measured in the capillary experiments. We note that when high shear was applied in the oscillatory shearing experiments, the complex viscosity of the blend abruptly increased and approached that of impact modifier, as the IM concentration reached a certain critical value. The experimentally observed effects of impact modifier on the rheology of the PMMA/IM blends were interpreted

considering possible physical interactions via entanglements of the acrylic shell molecules with the PMMA matrix molecules or other shell molecules. In addition, the dynamic shear measurements were compared with an emulsion model for immiscible blends by Palieme[12]. Significant deviations between the results from the dynamic shear experiments and the emulsion model applied are observed, and this may be due to the strong entanglements between the acrylic shell of the impact modifier particles and the PMMA matrix molecules. The discrepancy in the comparison of the dynamic shear measurements of the PMMA/IM blends between our experimental results and the emulsion model suggests that the complex dynamics of the PMMA/IM blends may not easily be described by the emulsion model in which the components are immiscible and the interfacial tension between the two phases is the only parameter which connects the phases. Any prediction of the complex dynamics of the multiphase blends with strong interactions between the components may require a new model in which the interactions such as entanglements between the phases are supplemented to the current emulsion models.

Symbols

α	: Interfacial tension
$\dot{\gamma}$: Shear rate
η	: Shear viscosity
$ \eta $: Complex viscosity
ϕ_i	: Volume fraction of the inclusions
ϕ	: Entire volume fraction of the dispersed phase
ω	: Frequency of Oscillation
G_m^*	: Complex modulus of the matrix
G_d^*	: Complex modulus of the dispersed phase
G_b^*	: Complex modulus of the blend
G'	: Storage modulus
G''	: Loss modulus
M_e	: Entanglement molecular weight in a binary blend
R_i	: Radius of the inclusions

References

1. C.B. Bucknall, Toughened Plastics, Applied Science Publishers, Ltd., 1977.
2. P.J. Burchill, Polymer 85: An International Symposium on Characterization and Analysis of Polymers, 1985, p. 116.
3. C. Keith Riew, Rubber Toughened Plastics, American Chemical Society, 1989.
4. C. Keith Riew, Toughened Plastics 1: Science and Engineering, American Chemical Society, 1993.
5. L. Shuca, *International Journal of Polymeric Materials*, **27**, 21

- (1994).
6. S. Havriliak, *Polymer International*, **25**, 67 (1991).
 7. S.Y. Hobbs, *Polymer Engineering and Science* **26**, 74 (1986).
 8. I.S. Miles and S. Rostami, *Multicomponent Polymer Systems*, Longman Scientific & Technical, Singapore, 1992.
 9. F. Haaf, H. Breuer, A. Echte, B.J. Schmitt, and J. Stabenow, *Journal of Science Industrial Research*, **40**, 659 (1981).
 10. C.J. Hooley, D.R. Moore, M. Whale, and M.J. Williams, *Plastics Rubber Process Applications*, **1** 345 (1981).
 11. P.A. Lovell, J. McDonald, D.E.J. Saunders, and R.J. Young, *Proceedings of PRI International Conference on Polymer Latex III*, 1989, p. 27.
 12. J.-F. Paliarne, *Rheological Acta*, **29**, 204 (1990).
 13. T.W. Hwang, Preparation of Multi-layered Acrylate Rubber Particles and Their Application to Toughening of Polymethylmethacrylate, Ph.D thesis, Seoul National University, Korea 1996.
 14. Y.L. Joo, J.Y. Hwang, and M.H. Cho, Proceeding of the 55th Annual Technical Conference, '97ANTEC 3 3045 (1997).
 15. J.G. Oldroyd, *Proceedings of Royal Society of London Series A*, **218** 122 (1953).
 16. S.J. Choi and W.R. Schowalter, *Physics of Fluids*, **18**, 420 (1975).
 17. P. Scholz, D. Froelich, and R. Muller, *Journal of Rheology*, **33**, 481 (1989).
 18. D. Graebing, R. Muller, and J.-F. Paliarne, *Marcromolecules*, **26**, 320 (1993).
 19. D. Graebing, A. Benkira, Y. Gallot, and R. Muller, *European Polymer Journal*, **30** 301 (1994).
 20. Y. Germain, B. Ernst, O. Genclot, and L. Dhamani, *Journal of Rheology*, **38**, 681 (1994).
 21. H. Gramspacher and J. Meissner, *Journal of Rheology*, **36**, 1127 (1992).
 22. M. Doi and T. Ohta, *Journal of Chemical Physics*, **95**, 1242 (1991).
 23. G.K. Guenther and D.G. Baird, *Journal of Rheology*, **40**, 1-20 (1996).
 24. H.M. Lee and O.O. Park, *Journal of Rheology*, **38**, 1405 (1994).
 25. A. Aji and L.A. Utracki, *Polymer Engineering and Science*, **36**, 1574 (1996).
 26. L.C. Sawyer and D.T. Grubb, *Polymer Microscopy*, Chapman and Hall, New York, 1987.
 27. P. Mariani, *Polymer Engineering and Science*, **36**, 2750 (1996).
 28. C.D. Han, *Multiphase Flow in Polymer Processing*, Academic Press, 1981.
 29. T. Matsuda, K. Kitagawa, and S. Onogi, *Polymer J.*, **1**, 418 (1970).
 30. J. Klein, D. Perahia, and S. Warburg, *Nature*, **352**, 143 (1991).
 31. J. Klein, E. Kumacheva, D. Mahalu, D. Perahia, and L.J. Fetters, *Nature*, **370**, 634 (1994).
 32. J. Klein, E. Kumacheva, D. Perahia, and S. Warburg, *Discuss Faraday Soc*, **98**, 173 (1994).
 33. P.S. Doyle, E.S.G. Shaqfeh, and A.P. Gast, *Physical Review Letters*, **78**, 1182 (1997).
 34. V. Kumaran, *Marcromolecules*, **26**, 2464 (1993).
 35. Y. Rubin and S. Alexander, *Europhysics Letter*, **13**, 49 (1990).
 36. J.-L. Barrat, *Marcromolecules*, **25**, 832 (1992).